Progress In Electromagnetics Research B, Vol. 6, 361–379, 2008

ANALYTICAL AND NUMERICAL ASPECTS OF BRAGG FIBER DESIGN

D. V. Prokopovich

Fiber Optics Research Center
38 Vavilov St., Moscow, 119991 Russia

A. V. Popov

Pushkov Institute of Terrestrial Magnetism
Ionosphere and Radio Wave Propagation
Troitsk, Moscow region, 142190 Russia

A. V. Vinogradov

Lebedev Physical Institute
53 Leninskij propsekt, Moscow, 119991 Russia

Abstract—Analytical theory and numerical approaches to the simulation and optimal design of multilayer mirrors and optical Bragg waveguides are developed. Optimal refractive index profiles in planar and cylindrical geometry are found. Reduction of the full set of Maxwell's equations to a scalar boundary value problem in the low-contrast approximation is discussed. An efficient finite-difference scheme is used to simulate realistic Bragg fibers.

1. INTRODUCTION

Along with holey fibers and other types of 2D photonic crystal waveguides, 1D band gap, or Bragg, structures are useful for visible or infrared light transmission, generation and amplification. The original idea [1] of holey Bragg fiber (BF) is still hardly realizable due to a great number of cladding layers needed for good mode confinement [2]. On the other hand, depressed core index BFs with just a few higher index layers demonstrate quasi single-mode behavior with large mode area and very low attenuation [3, 4]. Analysis shows that the BF

properties crucially depend on its refraction index profile characterized by thin high-index layers and sharp interfaces. Technology may impose limitations on the accuracy of reproducing theoretical profiles, which influences the resulting BF performance. In this context, two important mathematical problems arise:

(i) to find an optimum waveguide construction under certain technological constraints, and (ii) to develop an efficient, reliable and accurate mode solver capable to treat high-quality Bragg modes.

In this paper both aforementioned issues are addressed.

In Section 2, an analytical approach to the design of optimal multilayer mirrors and Bragg waveguides with maximum field confinement is developed. In Sections 3 and 4, radiative losses and dispersion of realistic Bragg waveguides are discussed and analytically estimated. Section 5 is devoted to the numerical simulation of realistic Bragg fibers by a finite-difference method. In Section 6, reduction of the full set of Maxwell's equations to a scalar boundary value problem is discussed and applied to realistic low-contrast Bragg waveguides.

2. PROBLEM OF MULTILAYER MIRROR OPTIMISATION

An optimal multilayer mirror should provide not only maximum reflectance but also a rapid field attenuation in the periodic structure. In fact, to have minimum number of layers is crucially important for practice. Let us find the optimal profile of the periodic refractive index $n(x) = n(x + \Lambda)$ providing maximum field decay over period Λ. The difficulty of this inverse problem lies in the absence of the analytical solution of the corresponding direct problem for an arbitrary $n(x)$. Consider the 1D wave equation to which Maxwell's equations are reduced in the simplest case of normal incidence of a plane wave on a multilayer structure. Let us write this equation for the transverse component of the electric field strength $E_y = u(x)$:

$$u'' + k^2 n^2(x) u = 0 \tag{1}$$

where $k = 2\pi/\lambda$ is the wave number of the incident wave. It turns out that the Floquet solution $u(x) = y(x)\exp(-\mu x),\ y(x) = y(x+2\Lambda)$, can be constructed in a closed form and an explicit formula for the decay decrement $\mu\Lambda$ can be obtained by introducing the parametrization

$$k^2 n^2(x) = f(p) \tag{2}$$

where $p = -u'/u$. This reduced (1) to a first-order equation

$$p' = p^2 + f(p) \tag{3}$$

having analytical solution

$$x(p) = \int \frac{dp}{p^2 + f(p)} + \text{const} \tag{4}$$

for an arbitrary function $f(p)$.

One can see from Figs. 1 and 2 that relation (2) is one-to-one mapping in the interval between the two successive zeros of the solution $u(x)$, where the parameter p increases from $-\infty$ to $+\infty$. The length of this interval is

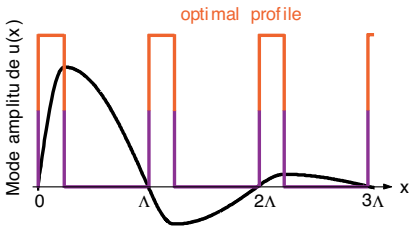

Figure 1. Electric field in periodic structure.

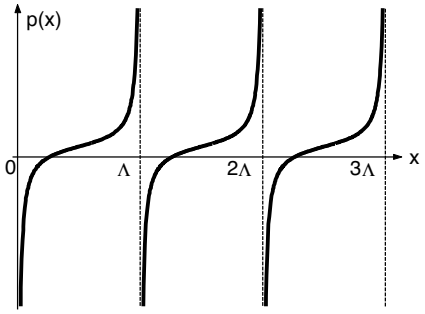

Figure 2. Logarithmic derivative $p(x) = -u'/u$.

$$\Lambda = \int_{-\infty}^{+\infty} \frac{dp}{p^2 + f(p)} \tag{5}$$

It is obvious that the solution

$$u(x) = C \exp\left(-\int p dx\right) = C \exp\left(-\int \frac{p dp}{p^2 + f(p)}\right) \tag{6}$$

constructed in this way can be periodically continued by matching at zeros $u(x) = 0$ $(x = \Lambda, 2\Lambda, \ldots)$, but the derivative $u'(x)$ would be discontinuous in this case. To provide smoothness of the solution, the function $u(x)$ must be multiplied by the ratio $u'(\Lambda)/u'(0)$ in each next period, which determines the required decay decrement

$$\mu\Lambda = \ln \frac{u'(0)}{u'(\Lambda)}$$

By differentiating expression (6), we obtain

$$\mu\Lambda = -\frac{1}{2} \int_{-\infty}^{+\infty} \frac{f'(p) dp}{p^2 + f(p)} \tag{7}$$

Figure 1 clarifies the relation between the field decay mechanism and asymmetry of $n(x)$ on the period Λ. Having found explicit expression (7) for the decrement $\mu\Lambda$, it is easy to formulate the condition for its maximization by using the classical theory of variational calculus. Because the Euler equation for integral (7) is degenerate and gives no solutions in the class of smooth functions $f(p)$, we transform the right-hand part of (7) to the form not containing the derivative $f'(p)$:

$$\begin{aligned}\mu\Lambda &= \lim_{R\to\infty}\left\{-\frac{1}{2}\int_{-R}^{+R}\frac{2p+f'(p)}{p^2+f(p)}dp+\int_{-R}^{+R}\frac{pdp}{p^2+f(p)}\right\}\\ &= V.P.\int_{-\infty}^{+\infty}\frac{dp}{p^2+f(p)}\end{aligned} \tag{8}$$

It is clear form physical considerations that the function $f(p) = k^2n^2(x)$ is limited and positive. Let us assume that $f_2 \le f(p) \le f_1,\ f_1, f_2 > 0$ (Fig. 3). The range of values of the integrand in (8) lies between the anti-symmetric curves drawn for constant functions f_1 and f_2 in Fig. 4. One can easily see that the maximum of the decay decrement is obtained by integrating the step function

$$f(p) = \begin{cases} f_1 & , \quad p<0 \\ f_2 < f_1 & , \quad p>0 \end{cases} \tag{9}$$

Taking into account (2) and (4), we obtain the optimal refractive index profile

$$\begin{aligned} n(x) &= \begin{cases} n_1, & 0<x<l_1 \\ n_2, & l_1<x<l_1+l_2=\Lambda \end{cases}, \\ l_1 &= \int_{-\infty}^{0}\frac{dp}{p^2+f_1}=\frac{\pi}{2kn_1}, \quad l_2=\int_{0}^{+\infty}\frac{dp}{p^2+f_2}=\frac{\pi}{2kn_2} \end{aligned} \tag{10}$$

and solution $u(x)$ (see Fig. 1). The maximum decrement is calculated from the expression (8):

$$\max(\mu\Lambda) = \ln\frac{n_1}{n_2} \tag{11}$$

The obtained meander refractive index profile (10) is well known in optics and corresponds to the so-called quarter-wave stack [5]. Thus, we have shown that a set of quarter-wave plates provides the absolute

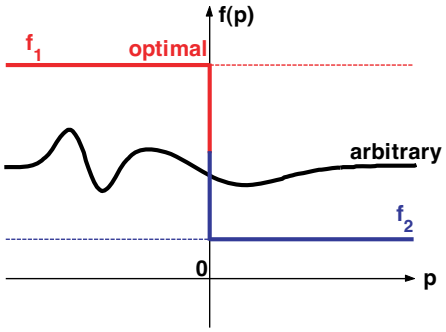

Figure 3. Arbitrary function $f(p)$ and step-wise optimal solution $f_{1,2}$ of the variational problem corresponding to maximum decay decrement.

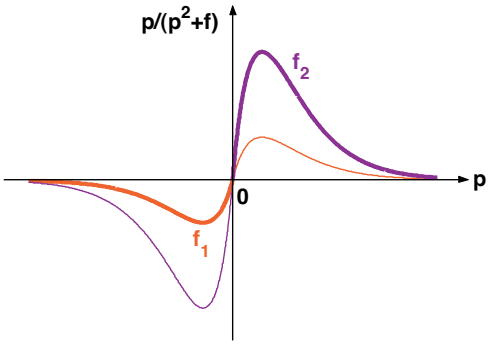

Figure 4. Integrand $p/(p^2 + f)$ in (8) for $f(p) = f_1$ and $f(p) = f_2$ (anti-symmetric curves), and its optimal value (thick curve).

maximum of the decay decrement not only for step structures [6] but also for an arbitrary periodic profile $n(x)$.

In practice, sharp boundaries between layers cannot be technologically produced, but the method described above can be also applied to maximization of the integral (8) with additional restrictions imposed on the derivative of the refractive index. For example, if the condition

$$\left|\frac{dn^2}{dx}\right| = \frac{1}{k^2}|f'(p)|[p^2 + f(p)] < \text{const} \tag{12}$$

is imposed, analysis shows that the maximum of the decrement $\mu\Lambda$ will be achieved at a piecewise linear function $n(x)$ (i.e., on a trapezoidal profile) and expressed in terms of the Airy function.

In the cylindrical case, scalar wave equation

$$u'' + \frac{1}{r}u' + k^2 n^2(r)u = 0 \tag{13}$$

can be used for qualitative estimations. An equation similar to (3) can be obtained by introducing parametrization $\vec{p} = -\nabla u/u$. Then

$$\nabla\vec{p} = \vec{p}^{\,2} - \frac{\Delta u}{u} = \vec{p}^{\,2} + f(\vec{r}, \vec{p}) \tag{14}$$

By using the properties of divergence in polar coordinates, denoting the rth component of the vector $\vec{p}$ as, $p_r = p(r)$ and assuming $p_\varphi = 0$, we get from (14)

$$p' + \frac{p}{r} = p^2 + f(r, p) \tag{15}$$

By making substitutions $\tilde{p} = p - 1/2r$ and $\tilde{f}(\tilde{p}) = f(r, p) + 1/4r^2$, we obtain the equation of type (3)

$$\tilde{p}' = \tilde{p}^2 + \tilde{f}(\tilde{p}) \tag{16}$$

and, thus, the cylindrical case is reduced to the one-dimensional problem.

The above analysis can be applied to the design of an optimum Bragg waveguide (BW). Consider first a planar case. Because the wave field in a periodic cladding of a planar BW is described by the equation of type (1)

$$u'' + [k^2 n^2(x) - \beta^2]u = 0 \tag{17}$$

where β is the longitudinal wave number of the propagating mode $E_y = u(x)\exp(i\beta z)$, the result obtained above gives immediately the optimal profile $n(x)$ providing maximum mode localization in the waveguide core. By replacing $n(x)$ with the effective refractive index $\sqrt{n^2(x) - \beta^2/k^2}$, we obtain from (10) the thickness of alternate layers in the periodic cladding, depending on the refractive indices n_1 and n_2 and the mode wave number β:

$$l_1 = \frac{\pi}{2\sqrt{k^2 n_1^2 - \beta_N^2}}, \qquad l_2 = \frac{\pi}{2\sqrt{k^2 n_2^2 - \beta_N^2}} \tag{18}$$

A discrete set of the optimal values of β_N is determined by the condition that the field amplitude vanishes on the internal boundary of the cladding and has the form

$$\beta_N^2 = k^2 n_0^2 - \frac{\pi^2}{a^2}\left(N + \frac{1}{2}\right)^2 \tag{19}$$

for the symmetric mode $u(x) = \cos x\sqrt{k^2 n_0^2 - \beta^2}$. Here, a is the half-thickness of the waveguide core, n_0 is the refractive index of the core, and N is the mode number.

For a cylindrical BW, due to similarity of Eqs. (16) and (3), the optimum profile $f(p)$ providing steepest mode decay in the cladding is step-function (9). This yields a quasi-periodic index distribution

$$n(x) = \begin{cases} \sqrt{n_1^2 - 1/4k^2 r^2}, & r_n < r < r_n + l_1 \\ \sqrt{n_2^2 - 1/4k^2 r^2}, & r_n + l_1 < r < r_n + \Lambda \end{cases} \tag{20}$$

where r_n are interfaces between high- and low-index layers. This optimal profile shown in Fig. 5 differs from the planar case by a small term $1/4k^2 r^2$ which must be taken into account only for fibers with small core radius $4k^2 a^2 \sim 1/\Delta n$. In most cases this correction can be neglected and we come to a purely periodic meander structure (10). This exact result agrees with the asymptotic theory of BF developed in [6, 7]: the electric field in the core is described by a Bessel function $J_m\left(r\sqrt{k^2 n_0^2 - \beta^2}\right)\cos m\varphi$, while in the cladding, Hankel asymptotics $\exp\left(\pm ir\sqrt{k^2\tilde{n}^2 - \beta^2}\right)/\sqrt{r}$ provide sufficient accuracy. The optimal cladding is a periodic quarter-wave step function starting from a zero of the Bessel function — see Fig. 5.

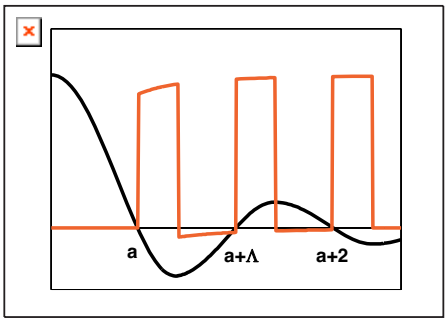

Figure 5. Optimal radial index profile and first Bragg mode.

For a given wavelength and core radius a, the cladding layers thicknesses are governed by Eq. (18) where the mode wave numbers are determined from the reduced dispersion equation $J_m\left(a\sqrt{k^2 n_0^2 - \beta^2}\right) = 0$ — zero amplitude at the core-cladding interface.

By considering a real BF, we face a number of problems complicating its optimization, such as technological restrictions related to the preparation of a perform and fiber drawing, the cylindrical rather then planar structure of the refractive index profile, necessity of studying parameters of a signal in a broad wavelength range. In this connection, an important problem is simulation of the mode structure, attenuation and dispersion in BFs with an arbitrary (theoretically specified or experimentally measured) refractive index profile.

3. PLANAR WAVEGUIDE WITH LEAKY MODES

In order to develop a numerical method for calculating BWs, we start from studying a planar model and then generalize the developed approach to real BFs. Consider a planar waveguide with periodically varying permittivity $\varepsilon = n^2(x)$.

Assuming that an electromagnetic wave propagates along the z axis and has only one electric field component $E_y = E(x, z)$. We obtain scalar wave equation

$$\frac{\partial^2 E}{\partial x^2} + \frac{\partial^2 E}{\partial z^2} + k^2 n^2 E = 0 \tag{21}$$

where $k = 2\pi/\lambda$ is the wave number in free space. We seek the solution of Eq. (21) in the form of a traveling wave $E(x, z) = u(x)\exp(i\beta z)$. In this case, Eq. (17), presented above, appears. It is convenient to represent the refractive index in the form $n^2(x) = \tilde{n}^2[1 + \alpha(x)]$, where $\alpha(\infty) = 0$, and $\tilde{n} = n(\infty)$. By representing the longitudinal wave vector in the form $\beta = \tilde{k}\sqrt{1-\gamma^2}$, where $\tilde{k} = k\tilde{n}$, and $\gamma = \sin\theta$ is the sine of the mode glancing angle, we write (17) in a convenient form

$$u'' + \tilde{k}^2[\alpha(x) + \gamma^2]u = 0 \tag{22}$$

The boundary conditions for a symmetric solution of Eq. (22) are vanishing of the derivative at the origin and the radiative behavior at infinity:

$$u'(0) = 0, \quad u(x) \propto T\exp(i\tilde{k}\gamma x) \quad (x \to \infty) \tag{23}$$

By solving Eq. (22) with boundary conditions (23), we obtain the mode spectrum of planar BW under study, i.e., a discrete set of the eigenvalues γ and eigenfunctions $u(x;\gamma)$. Generally speaking, the quantities γ and β are complex, and by introducing the notation $\beta = \beta' + i\beta''$, and $\gamma = \gamma' - i\gamma''$, we obtain, in the absence of absorption ($\mathrm{Im}n = 0$), the equality $\beta'\beta'' = \tilde{k}^2\gamma'\gamma''$. The modes for which $\beta' \geq 0$

(i.e., propagating in the positive direction of z axis) and $\beta'' \geq 0$ have the physical sense; therefore, it follows from the condition

$$\beta' \geq 0, \quad \beta'' \geq 0 \rightarrow \gamma'\gamma'' \geq 0 \tag{24}$$

i.e., γ' and γ'' have the same sign. Thus, a leaky mode proportional to $\exp(i\tilde{k}\gamma x)$ and propagating in the positive direction of the transverse coordinate x (width $\gamma' \geq 0$) will increase at infinity (because $\gamma'' \geq 0$). We will call Bragg modes the weakly decaying solutions localized in the core, for which the relation

$$|\beta''| \ll |\beta'| \tag{25}$$

is fulfilled. Losses expressed in $\mathrm{dB}\times\mathrm{km}^{-1}$ in fiber optics, are

$$A = \frac{20 \times 10^9}{\log 10}\beta'' \tag{26}$$

where β'' is measured in $\mu\mathrm{m}^{-1}$.

The important characteristics of a fiber is the wavelength dependence of the Bragg mode losses and chromatic dispersion [8]

$$D = -\frac{k^2}{2\pi c}\frac{\partial^2\beta'}{\partial k^2} \tag{27}$$

where D is measured in $\mathrm{ps}\cdot\mathrm{nm}^{-1}\cdot\mathrm{km}^{-1}$.

4. BRAGG MODE RADIATION LOSS

In a realistic BF, the periodic cladding is surrounded with an outer coating of constant refraction index $\tilde{n}$. If $\tilde{n} > n_0$, the Bragg mode exhibits small leakage through the finite number of cladding layers, which results in exponential decay along the waveguide axis z. The attenuation rate is proportional to the imaginary part of the mode wave number $\beta = \beta' + i\beta''$. In the planar waveguide model, it can be found from the exact relation

$$\beta'' = \frac{[u'(b)u*(b) - u(b)u'*(b)]}{4i\beta' \int\limits_0^b |u(x)|^2 dx} = \frac{\mathrm{Re}\,\tilde{q}|u(b)|^2}{2\beta' \int\limits_0^b |u|^2 dx} \tag{28}$$

following from matching the modal solution $u(x)$ with the outgoing wave $T\exp(i\overline{q}x)$ at the outer cladding boundary $x = b$. Here,

$\tilde{q} = \sqrt{k^2\tilde{n}^2 - \beta^2}$ is the complex-valued transverse wave number to be found from a general dispersion equation.

Assuming small leakage, we can avoid solving the dispersion equation and get an explicit asymptotic formula for the optimal mode radiation loss. To the first approximation, the wave field in the cladding is proportional to the decreasing Floquet solution

$$u(x) = \begin{cases} (-1)^n A_n \sin q_1(x - x_n), & x_n < x < x_n + l_1 \\ (-1)^n A_n \cos q_2(x - x_n - l_1), & x_n + l_1 < x < x_n + \Lambda \end{cases} \quad (29)$$

Here, $q_{1,2} = \sqrt{k^2 n_{1,2}^2 - \beta^2}$ — transverse wave numbers in alternate high- and low-index layers, $l_{1,2}$ are the layer thicknesses defined in Eq. (18), and the amplitudes A_n decay in geometric progression: $A_{n+1} = A_n q_2/q - 1$. Furthermore, as the correction to the wave solution due to the finite number of layers is very small at the core-cladding interface, we can put into the above formulas the unperturbed value $\beta' \simeq \beta$, where β is defined from Eq. (19). Finally, evaluating the mode intensity $|u(b)|^2$ at the end of $N + 1/2$ bilayer cladding and the integral in the denominator of (28) we obtain the sought estimate of the optimal mode radiation loss

$$\beta'' = \frac{\sqrt{k^2\tilde{n}^2 - \beta'^2}}{\beta'} \left(\frac{l_1}{a}\right)^2 \left(\frac{l_1}{l_2}\right)^{2N} \frac{1/l_1^2 - 1/l_2^2}{a\,(1/l_1^2 - 1/l_2^2) + (l_1 + l_2)/a^2} \quad (30)$$

For a large number of bi-layers N, the main factor determining the radiation loss is $(l_1/l_2)^{2N}$ which gives a rough qualitative estimate of the mode quality dependence on the BF parameters. A more accurate estimation based on the formula (30) is presented in the contour plot of Fig. 6, while BF cross-section structure versus a/λ ratio is visualized in Fig. 7. This formula exactly holds for the optimal cylindrical BF as well; a similar derivation takes into account absorption in the cladding material.

5. FINITE-DIFFERENCE SCHEME FOR SOLVING THE BOUNDARY VALUE PROBLEM

Let us construct a finite-difference (FD) scheme for solving boundary value problem (22), (23). After the substitution $u(x) = w(x)\exp(i\tilde{k}\gamma x)$, Eq. (22) takes the form

$$w'' + 2i\tilde{k}\gamma w' + \tilde{k}^2\alpha(x)w = 0 \quad (31)$$

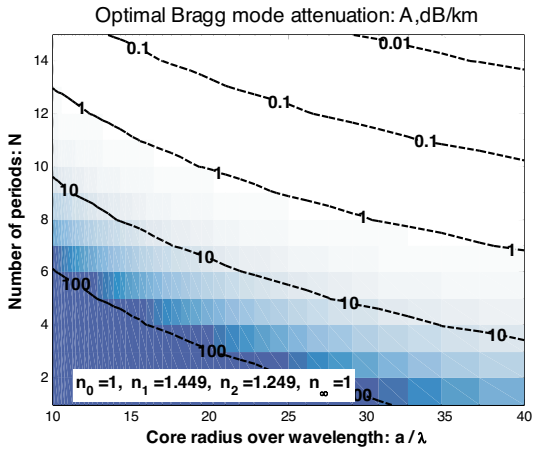

Figure 6. Bragg mode radiation loss as a function of BF parameters and wavelength.

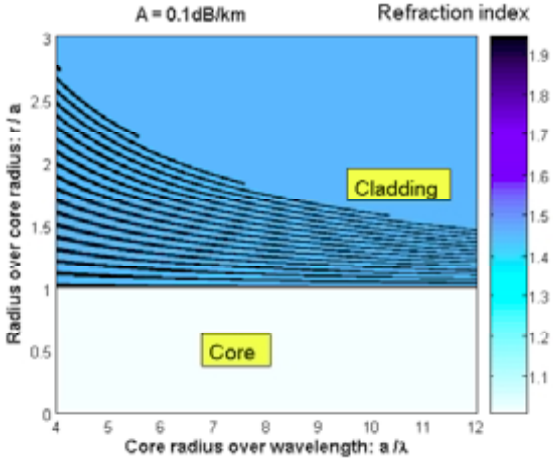

Figure 7. Cross sections of optimal BF providing Bragg mode attenuation.

Note that, unlike initial Eq. (22), spectral parameter γ enters linearly into Eq. (31). Boundary conditions are transformed to the relations

$$w'(0) + i\tilde{k}\gamma w(0) = 0, \quad w'(R) = 0 \tag{32}$$

where R is the linear size of the region on which the FD scheme is constructed. The parameter γ enters linearly into both Eqs. (31) and (32), which considerably simplifies the formulation of the eigenvalue

problem. Introducing FD grid ($x_m = mh \in [0; R],\ m = 0, 1, \ldots, M$) for Eq. (31) and adding extra nodes with $m = -1,\ M + 1$, we obtain a difference analogue of Eq. (31):

$$\frac{w_{m+1} - 2w_m + w_{m-1}}{h^2} + i\tilde{k}\gamma\frac{w_{m+1} - w_{m-1}}{h} + \tilde{k}^2\alpha_m w_m = 0 \qquad (33)$$

where $m = 0, 1, \ldots, M;\ w_m = w(x_m)$ and $\alpha_m = \alpha(x_m)$. Equation (33) can be rewritten in the vector form

$$\boldsymbol{A}\vec{w} = i\mu\boldsymbol{B}\vec{w} \qquad (34)$$

where the notation $\mu = \tilde{k}h\gamma$, $q_m = \tilde{k}^2h^2\alpha_m$, $\vec{w} = \{w_m\}$ and $(M + 1) \times (M + 1)$ matrices

$$\boldsymbol{A} = \begin{Vmatrix} 1 & 0 & -1 & \cdots & \cdots & 0 & 0 \\ 1 & q_1 - 2 & 1 & & & \iddots & 0 \\ \vdots & \ddots & \ddots & \ddots & & & \vdots \\ \vdots & & 1 & q_m - 2 & 1 & & \vdots \\ \vdots & & & \ddots & \ddots & \ddots & \vdots \\ 0 & \iddots & & & 1 & q_{M-1} - 2 & 1 \\ 0 & 0 & \cdots & \cdots & \cdots & 2 & q_M - 2 \end{Vmatrix},$$

$$\boldsymbol{B} = \begin{Vmatrix} 0 & 2 & \cdots & \cdots & \cdots & 0 & 0 \\ 1 & 0 & -1 & & & \iddots & 0 \\ \vdots & \ddots & \ddots & \ddots & & & \vdots \\ \vdots & & 1 & 0 & -1 & & \vdots \\ \vdots & & & \ddots & \ddots & \ddots & \vdots \\ 0 & \iddots & & & 1 & 0 & -1 \\ 0 & 0 & \cdots & \cdots & \cdots & 0 & 0 \end{Vmatrix}$$

are introduced. Thus, the solution of the differential equation (31) is reduced to a linear algebraic eigenvalue problem. Equation (34) has $M + 1$ solutions (FD modes): $\mu_m, \{w_m^{(t)}\}\ m = 0, 1, \ldots, M$. The modes of the differential equation (31), being of interest to us, are separated from the total set of solutions by the condition of finite limit $\lim\limits_{h\to 0}(\gamma) = \lim\limits_{h\to 0}(\mu/\tilde{k}h)$ when the grid step tends to zero. It must be noted that all kinds of BW modes are taken into account in this approach: modes trapped in the cladding rings, surface modes and leaky modes

weakly confined in the core due to the interference reflection from the periodical cladding. To find the high-quality Bragg modes, we use the criterion of low losses (25) supplemented with the condition of mode localization in the fiber core:

$$\int_0^a |u(x)|^2 dx > \int_a^R |u(x)|^2 dx \tag{35}$$

The results of the numerical solution of Eq. (34) are presented in Figs. 8 and 9 (1st and 2nd even modes and the wavelength dependence of radiative losses) for a waveguide with the following parameters of the refractive index profile: $a = 24.23\,\mu$m, $l_1 = 1.4\,\mu$m, $l_2 = 6.75\,\mu$m, $l_3 = 1.47\,\mu$m, $l_4 = 6.66\,\mu$m, $l_5 = 1.49\,\mu$m; $n_0 = 1.4485$, $n_1 = 1.459$, $n_2 = 1.449$, $n_3 = n_1$, $n_4 = n_2$, $n_5 = n_1$, $\tilde{n} = n_2$.

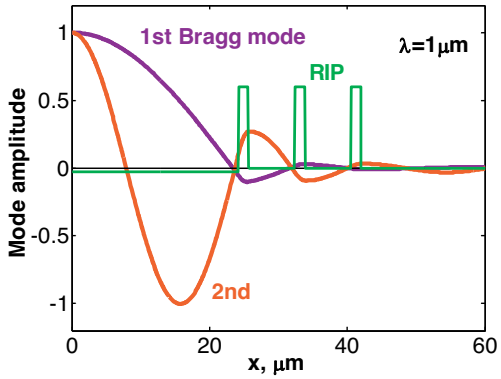

Figure 8. Amplitude of two lowest Bragg even modes for $\lambda = 1\,\mu$m calculated by solving numerically Eq. (34).

6. MAXWELL'S EQUATIONS AND SCALAR APPROXIMATION FOR A BF

Consider a cylindrical waveguide with the radial permittivity profile $\varepsilon(r)$. We seek the electromagnetic field of a travelling wave in the form $\vec{E}(r,\varphi)\exp(i\beta z)$ and $\vec{H}(r,\varphi)\exp(i\beta z)$. The system of wave equations in cylindrical coordinates for the transverse component E_r and E_φ obtained from Maxwell's equation has the form

$$\frac{\partial^2 E_r}{\partial r^2} + \left(\frac{1}{r} + \frac{\varepsilon'}{\varepsilon}\right)\frac{\partial E_r}{\partial r} + \left[k^2\varepsilon - \beta^2 - \frac{1}{r^2} + \left(\frac{\varepsilon'}{\varepsilon}\right)'\right] E_r + \frac{1}{r^2}\frac{\partial^2 E_r}{\partial \varphi^2}$$

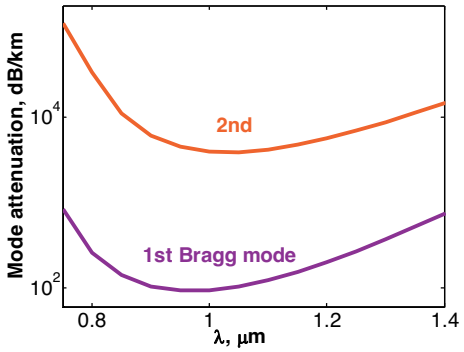

Figure 9. Wavelength dependence of mode attenuation in a planar waveguide calculated by solving numerically Eq. (34).

$$\begin{aligned} &= \frac{2}{r^2}\frac{\partial E_\varphi}{\partial \varphi} \\ &\frac{\partial^2 E_\varphi}{\partial r^2} + \frac{1}{r}\frac{\partial E_\varphi}{\partial r} + \left[k^2\varepsilon - \beta^2 - \frac{1}{r^2}\right] E_\varphi + \frac{1}{r^2}\frac{\partial^2 E_\varphi}{\partial \varphi^2} \\ &= -\left(\frac{2}{r^2} + \frac{\varepsilon'}{r\varepsilon}\right)\frac{\partial E_r}{\partial \varphi} \end{aligned} \tag{36}$$

Vector angular harmonics $E_r = P_l(r)\sin l\varphi$ and $E_\varphi = Q_l(r)\cos l\varphi$ ($l = 0, 1, \ldots$) are determined by the set of coupled equations

$$\begin{cases} P_l'' + \left(\dfrac{1}{r} + \dfrac{\varepsilon'}{\varepsilon}\right) P_l' + \left[k^2\varepsilon - \beta^2 - \dfrac{l^2+1}{r^2} + \left(\dfrac{\varepsilon'}{\varepsilon}\right)'\right] P_l = -\dfrac{2l}{r^2} Q_l \\ Q_l'' + \dfrac{1}{r} Q_l' + \left(k^2\varepsilon - \beta^2 - \dfrac{l^2+1}{r^2}\right) Q_l = -l\left(\dfrac{2}{r^2} + \dfrac{\varepsilon'}{r\varepsilon}\right) P_l \end{cases} \tag{37}$$

High-quality Bragg modes are close in form to the modes of hollow metallic waveguide [9], which can be verified by making the substitution

$$\begin{cases} P_l = u_l(r) + v_1(r) \\ Q_l = u_l(r) - v_1(r) \end{cases} \tag{38}$$

Functions $u_l(r)$ and $v_l(r)$ satisfy the following equations

$$\begin{cases} u_l'' + \dfrac{1}{r}u_l' + \left(k^2\varepsilon - \beta^2 - \dfrac{(l-1)^2}{r^2}\right)u_l = -\dfrac{1}{2r^l}\left(\dfrac{r^l\varepsilon'}{\varepsilon}P_l\right)' \\ v_l'' + \dfrac{1}{r}v_l' + \left(k^2\varepsilon - \beta^2 - \dfrac{(l+1)^2}{r^2}\right)v_l = -\dfrac{r^l}{2}\left(\dfrac{\varepsilon'}{r^l\varepsilon}P_l\right)' \end{cases} \tag{39}$$

This set decouples for $\varepsilon'(r) = 0$ (for example, in the homogeneous core of a BW) into two independent equations. In the case of a weak dielectric contrast, of interest to us: ($\varepsilon = \tilde{n}^2[1 + \alpha(r)]$, $|\alpha(r)| \ll 1$) equations (39) are weakly coupled in the quasi-periodic cladding of the waveguide. In the zero-order approximation, the right-hand side of the first equation in (39) can be neglected; in this case, two independent series of the eigenvalues β_{ln} appear corresponding to the eigenfunctions $\left\| \begin{matrix} u_{ln} \\ 0 \end{matrix} \right\|$ and $\left\| \begin{matrix} 0 \\ v_{ln} \end{matrix} \right\|$ where $n = 1, 2, \ldots$. Corrections taking into account a weak coupling of Eq. (39) can be found by the perturbation theory [10].

Cartesian components of the transverse electric field have the form

$$\begin{cases} E_x = u_l \sin(l-1)\varphi + v_l \sin(l+1)\varphi \\ E_y = u_l \cos(l-1)\varphi - v_l \cos(l+1)\varphi \end{cases} \tag{40}$$

In the most interesting case of $l = 1$, a fundamental mode appears which has axially symmetric field distribution with a small "impurity" of the quadruple harmonic: $E_y = u_1(r) - v_1(r)\cos 2\varphi$, $E_x = v_1(r)\sin 2\varphi$ ($|v_1| \ll |u_1|$). By neglecting the quadruple components and denoting $u_1(r) = u(r)$, we arrive at the scalar wave equation

$$u'' + \frac{1}{r}u' + \tilde{k}^2[\alpha(r) + \gamma^2]u = 0 \tag{41}$$

describing linearly polarized modes of the BW in the low-constant approximation ($|\varepsilon'/\varepsilon| \ll 1$). Regular solutions of (41) in the homogeneous core are zero-order Bessel functions $u(r) = J_0\left(\tilde{k}r\sqrt{\alpha_0 + \gamma^2}\right)$ having a maximum on the waveguide axis, which gives the first boundary condition

$$u'(0) = 0 \tag{42}$$

The solution of Eq. (41) in the homogeneous external coating behaves as the Hankel function of the first kind, i.e., $u(r) = TH_0^{(1)}(\tilde{k}\gamma r)$, $T =$

const. Eliminating the coefficient T we obtain the second boundary condition

$$\frac{u'(R)}{u(R)} = -\tilde{k}\gamma \frac{H_1^{(1)}(\tilde{k}\gamma R)}{H_0^{(1)}(\tilde{k}\gamma R)} \tag{43}$$

The boundary-value problem (41)–(43) is similar to the eigenvalue problem considered in Section 3 by studying the modes of a planar BW. The difference is that Eq. (39) contains an addition singular term u'/r, and the radiation condition (43) is more complicated. Substitution $u(r) = w(r)\exp(i\tilde{k}\gamma r)$ and replacement of the Hankel functions in (43) by their asymptotics reduces the boundary-value problem to an equivalent form

$$\begin{aligned} &w'' + \frac{1}{r}w' + 2i\tilde{k}\gamma\left(w' + \frac{w}{2r}\right) + \tilde{k}^2\alpha w = 0 \\ &w'(0) = -i\tilde{k}\gamma w(0), \quad w'(R) \approx -\frac{1}{2R}w(R) \end{aligned} \tag{44}$$

which contains, unlike (41), γ to the first power. The equations (44) admit a simple FD approximation and can be solved by standard methods of linear algebra, similarly to the solution of Eq. (34) considered above.

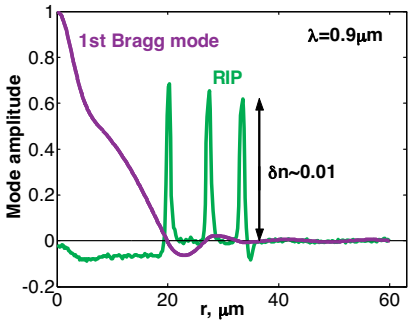

Figure 10. Amplitude $u(r)$ of the first Bragg mode for bare BF-541 at $\lambda = 0.9\,\mu$m.

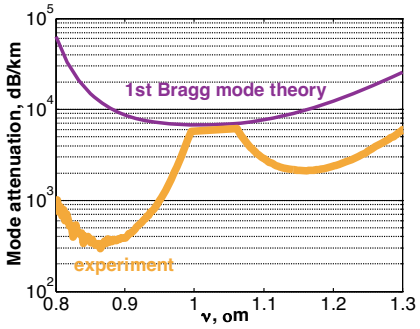

Figure 11. Bragg mode attenuation vs wavelength for bare BF-541: numerical calculation and experiment [11].

Figures 10 and 11 present the results of numerical simulation of the mode amplitude and radiation losses for a real BF-541 fabricated at the RAS Fiber Optics Research Center [11]. First comparisons revealed a striking discrepancy between the theoretical and experimental loss spectra (Fig. 11). It has been pointed out in a recent paper [12]

that this discrepancy is explained by the unaccounted influence of the protective polymer jacket surrounding the fiber, resulting in additional resonance effects. Further calculations confirmed this conclusion.

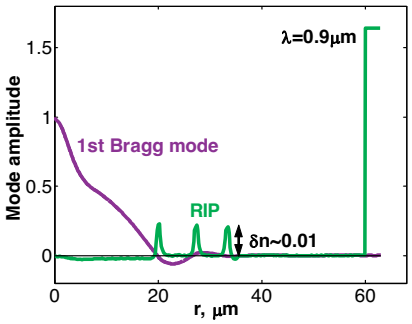

Figure 12. Amplitude $u(r)$ of the first Bragg mode for BF-541: polymer jacket taken into account.

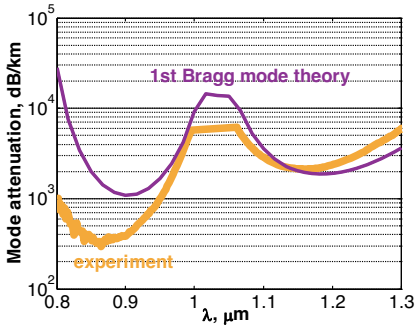

Figure 13. Bragg mode attenuation vs wavelength for BF-541: polymer jacket taken into account.

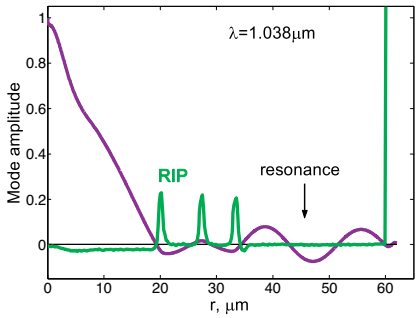

Figure 14. Resonance effect appearing in the region between Bragg rings and polymer jacket for $\lambda = 1.038\,\mu$m.

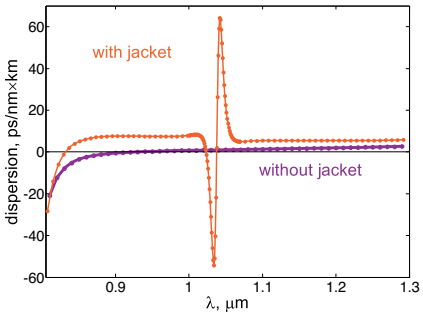

Figure 15. Wave dispersion D calculated via Eq. (27) for bare BF-541 without jacket and with a polymer jacket.

Figs. 12 and 13 show the calculated first Bragg mode and its loss spectrum for the same BF surrounded by a polymer jacket with a higher refractive index ($n_{pol} = 1.52$). One can see that, for almost invariable field distribution in core at $0.9\,\mu$m, the losses at this wavelength decreased almost by an order of magnitude, whereas at $1.038\,\mu$m a local maximum was observed instead of the loss minimum. This maximum can be explained by energy transfer to a circular mode concentrated between the Bragg rings and the polymer jacket

(Fig. 14). Qualitatively, the calculated loss spectrum agrees well with experimental results. To obtain a complete quantitative agreement, more accurate data on the refractive index and absorption in the jacket are required. Figure 15 shows the wave dispersion calculated for the BF-541. One can see that the dispersion of the bare waveguide without jacket is small and linearly increases in a broad wavelength range. The influence of the polymer jacket manifests in a drastic dispersion increase and change of sign in the region of the resonance loss maximum.

7. CONCLUSION

We have proposed an analytic method for optimizing a multilayer mirror. It has been shown that a stack of quarter-wave layers provides the absolute maximum of the decay decrement not only for step structures but also for an arbitrary periodic refractive index profile.

Realistic Bragg fibers are simulated by solving numerically the scalar wave equation with radiation condition at infinity. A complete complex spectrum of the Bragg fiber modes describing guided and leaky modes has been found. The developed finite-difference method for mode calculation reduces the boundary-value problem to an eigenvalue problem which can be solved by standard methods of linear algebra.

It has been shown that the scalar approximation of Maxwell's equations in cylindrical coordinates for Bragg fibers with weak refractive index contrast in the periodic cladding provides a good agreement with experimental results.

ACKNOWLEDGMENT

This work was supported by the Russian Foundation for Basic Research (Grant No. 07-02-01244-a).

REFERENCES

1. Yeh, P., A. Yariv, and E. Marom, "Theory of Bragg fiber," *J. Opt. Soc. Am.*, Vol. 68, No. 9, 1196–1201, 1978.
2. Popov, A. V., A. V. Vinogradov, R. M. Fechtchenko, Yu. A. Uspenskii, and E. M. Dianov, "Qualitative theory and modeling of hollow Bragg waveguides," *ICTON 2003 Conf. Proc.*, Vol. 1, 206–211, Warsaw, 2003.

3. Février, S., P. Viale, F. Gerome, P. Leproux, P. Roy, J.-M. Blondy, B. Dussardier, and G. Monnom, "Very large effective area singlemode photonic bandgap fiber," *Electron. Lett.*, Vol. 39, No. 17, 1240–1242, 2003.
4. Fevrier, S., S. Semjonov, V. Khopin, et al., "Low loss large mode area Bragg fibre," *Proc. of 31th ECOC*, Th. 4.4.3, Glasgow, UK, 2005.
5. Born, M. and E. Wolf, *Principle of Optics*, Pergamon Press, Oxford, 1969.
6. Xu, Y., R. K. Lee, and A. Yariv, "Asymptotic analysis of Bragg fibers," *Opt. Letters*, Vol. 25, 1756–1758, 2000.
7. Xu, Y., et al., "Asymptotic analysis of silicon based Bragg fibers," *Opt. Express*, Vol. 11, 1039–1049, 2003.
8. Ramaswami, R. and K. N. Sivarajan, *Optical Networks: A Practical Perspective*, Academic Press, London, 1998.
9. Johnson, S. G., M. Ibanescu, M. Skorobogatiy, O. Weisberg, T. D. Engeness, M. Soljacic, S. A. Jacobs, J. D. Joannopulos, and Y. Fink, "Low-loss asymptotically single-mode propagation in large-core OmniGuide fibers," *Opt. Express*, Vol. 9, No. 13, 748–779, 2001.
10. Landau, L. D. and E. M. Lifshits, *Quantum Mechanics: Non-relativistic Theory*, Pergamon Press, London, 1977.
11. Jamier, R., P. Viale, S. Fevrier, J. M. Blondy, S. L. Semjonov, M. E. Likhachev, M. M. Bubnov, E. M. Dianov, V. F. Khopin, M. Y. Salganskii, and A. N. Guryanov, "Depressed-index-core singlemode bandgap fiber with very large effective area," *OFC/NFOEC'2006 Tech. Digest*, Anaheim, California, USA, 2006.
12. Uspenskij, Yu. A., M. E. Likhachev, S. L. Semjonov, M. M. Bubnov, E. M. Dianov, E. E. Uzorin, O. S. Simokhin, A. V. Vinogradov, R. Jamier, S. Février, and J.-M. Blondy, "Effect of polymer coating on leakage losses in Bragg fibers," *Opt. Letters*, Vol. 32, 1202, 2007.